Spiroplasma eriocheiris FtsZ assembles the ring-like structure assisted by SepF

Received for publication, October 17, 2024, and in revised form, February 11, 2025 Published, Papers in Press, March 4, 2025,
https://doi.org/10.1016/j.jbc.2025.108373

Taishi Kasai[1], **Yuhei O. Tahara**[2,3], **Makoto Miyata**[2,3], **and Daisuke Shiomi**[1,*]

From the [1]*Department of Life Science, College of Science, Rikkyo University, Tokyo, Japan;* [2]*Graduate School of Science, Osaka Metropolitan University, Osaka, Japan;* [3]*The OMU Advanced Research Center for Natural Science and Technology, Osaka Metropolitan University, Osaka, Japan*

Reviewed by members of the JBC Editorial Board. Edited by Enrique De La Cruz

The FtsZ protein is involved in bacterial cell division. In cell-walled bacteria, such as *Bacillus subtilis*, FtsZ forms a ring-like structure, called the Z ring, at the cell division site and acts as a scaffold for cell wall synthesis. The inhibition of cell wall synthesis in *B. subtilis* has been shown to interfere with the function of the Z ring, causing a loss in cell division control. *Spiroplasma*, a cell wall-less bacterium, lacks most of the genes involved in cell division; however, the *ftsZ* gene remains conserved. The function of *Spiroplasma eriocheiris* FtsZ (SeFtsZ) remains to be determined. In the present study, we analyzed the biochemical characteristics of SeFtsZ. Purified SeFtsZ demonstrated lower polymerization capacity and GTPase activity than FtsZ from *Escherichia coli* and *B. subtilis*. We also investigated the relationship between SeFtsZ and SeSepF, which anchors FtsZ to the cell membrane, and found that SeSepF did not contribute to the stability of FtsZ filaments, unlike the *B. subtilis* SepF. SeFtsZ and SeSepF were produced in *E. coli* L-forms, where cell wall synthesis was inhibited. SeFtsZ formed ring-like structures in cell wall-less *E. coli* cells, suggesting that SeFtsZ forms Z rings and is involved in cell division independently of cell wall synthesis.

Bacteria generally divide in the middle of the cell. The cell division apparatus complex called the Z ring, of which FtsZ is a major component, must be correctly localized at the division site. FtsZ is a tubulin homolog consisting of a globular tubulin-like domain containing GTP-binding and GTPase domains, an H7 domain that connects GTP-binding and GTPase domains, a T7 loop, an intrinsically disordered C-terminal "linker," and a C-terminal tail which is a highly conserved ∼11 residues region responsible for the interaction with other proteins (1, 2). The T7 loop from one FtsZ subunit is inserted into the GTP-binding site of the next, inducing GTP hydrolysis (3). The tense state (T-state) of FtsZ bound to GTP polymerizes to form filaments. FtsZ hydrolyzes GTP in the filament, changing it to the relaxed state (R-state); in turn, the filament becomes destabilized and depolymerized (4). Leucine residue at the 272 position in the FtsZ globular domain in *Escherichia coli* is homologous to residue involved in the longitudinal contact of β-tubulin (5, 6). When this residue is mutated to glutamate (L272 E), FtsZ fails to polymerize and loses its GTPase activity (7, 8).

In *Bacillus subtilis*, the Z ring localization at mid-cell is determined by nucleoid occlusion and the Min system (9, 10). Noc is a protein involved in nucleoid occlusion (11, 12). It is thought to recruit chromosomes to the cell membrane and physically prevent the assembly of the cell division machinery near the nucleoid (13). In contrast, MinC prevents the assembly of the cell division machinery at the cell poles (14). The Z ring is anchored to the cell membrane by FtsA and SepF, which interact with the C-terminus of FtsZ and stabilize its filament (15, 16). The actin homolog FtsA has an amphipathic helix at its C-terminus, a membrane-bound region, and SepF is self-assembled and forms a ring structure (17–20). The SepF ring bundles FtsZ filaments and transforms them into tube-like structures (18). Glycine residues at positions 109 and 116 of SepF in *B. subtilis* are important for interacting with FtsZ (Fig. S1) (18). Gly109 also affects intermolecular interactions with SepF dimers (18). Once anchored to the cell membrane, the Z-ring assembles with other cell division proteins to form the complex 'divisome,' which acts as a scaffold for cell wall synthesis (21, 22). FtsW and PBP2B function as a transglycosylase and transpeptidase, respectively (23, 24). FtsL, DivIB, and DivIC form complexes involved in the localization of FtsW and PBP2B to the Z ring (25).

In cell-walled bacteria, such as *B. subtilis*, cell-wall synthesis is linked to cell division since the dividing site must be filled with a new cell wall (26, 27). Cell wall synthesis inhibition has been shown to interfere with the function of cell division proteins. For example, when cell wall synthesis is inhibited by β-lactam antibiotics, such as penicillin, *E. coli* and *B. subtilis* cells are lysed since β-lactams inhibit the activity of penicillin-binding proteins (PBPs), which crosslinks the peptides in peptidoglycan (28). However, under hyperosmotic conditions, although most cells are lysed owing to the inhibition of cell wall synthesis by antibiotics or lysozymes, some cells are transformed into a viable state without a cell wall, referred to as the L-form (29). In the L-forms, FtsZ is not required for cell division, and the elongated cell membranes divide irregularly (30). However, even in *E. coli* L-forms, the Z ring is formed but does not constrict, indicating that peptidoglycan or its synthesis is required for the constriction of the Z ring (31).

* For correspondence: Daisuke Shiomi, dshiomi@rikkyo.ac.jp.

Consistently, *E. coli* FtsZ inside liposomes forms Z-rings that do not split liposomes (32). Therefore, FtsZ-regulated cell division in cell-walled bacteria may require the cell wall. However, some bacteria, such as *Mycoplasmas*, are not originally surrounded by a cell wall. Some mycoplasmas and related species encode the *ftsZ* and *sepF* genes in their genomes, although these species lack most of the genes involved in cell wall synthesis (33–36). *ftsZ* deficiency in *Mycoplasma* affects cell morphology and division rates (37). Synthetic bacterium JCVI-Syn3.0, which has the smallest genome derived from *Mycoplasma*, showed an increased growth rate when several genes, including *ftsZ* and *sepF*, were introduced (38). Therefore, *Mycoplasma* FtsZ may function differently from the FtsZ of *E. coli* and *B. subtilis*. However, data regarding cell division in bacteria without cell walls, other than in cell-walled bacteria such as *E. coli* or *B. subtilis*, and the regulation of FtsZ localization and its functions during cell division remain limited.

The function of cytoskeletal proteins is altered in *Spiroplasma*, a close relative of *Mycoplasma*. In this study, we investigated the role of FtsZ and SepF in *Spiroplasma* cell division and, using purified FtsZ and SepF of *Spiroplasma eriocheiris* (SeFtsZ and SeSepF), determined the biochemical properties and structure of SeFtsZ. We also used walled or wall-deficient (L-form) *E. coli* cells to observe the behavior of SeFtsZ in cells.

Results

GTP-dependent polymerization of Spiroplasma *FtsZ*

His_6-SeFtsZ and His_6-SeSepF (hereafter referred to as SeFtsZ and SeSepF, respectively, unless otherwise indicated) were overproduced in *E. coli* and purified using His-tag affinity chromatography. *SesepF* gene (NZ_CP011856) was identified using PSI-BLAST based on the amino acid sequence of *B. subtilis* SepF. To analyze the polymerization of SeFtsZ, purified SeFtsZ was incubated in a polymerization buffer with GTP or GDP for 30 min. Samples were fractionated *via* ultracentrifugation. The amount of SeFtsZ in the supernatant and pellet fractions was estimated from the bands of Coomassie brilliant blue (CBB)-stained SDS-PAGE gel (Fig. 1). Almost all SeFtsZ was detected in the supernatant in the presence of GDP, whereas 16% of SeFtsZ was retrieved from the pellet in the presence of GTP, consistent with previous findings (39, 40). Next, the effect of SeSepF on SeFtsZ polymerization was examined. Purified SeFtsZ was mixed with purified SeSepF in polymerization buffer for 5 min. The mixed solution was then incubated with GTP or GDP for 30 min. Almost all SeFtsZ and SeSepF were detected in the supernatant in the presence of GDP. In the presence of GTP, 28% of SeFtsZ was retrieved from the pellet fraction, suggesting that SeSepF promotes the polymerization of SeFtsZ.

To confirm that the increase in SeFtsZ sedimentation was attributed to the interaction between SeFtsZ and SeSepF, we first examined the interaction between SeFtsZ and SeSepF using bio-layer interferometry. Before the analysis, the His-tag of SeFtsZ was removed since one of the His-tagged protein (His_6-SeSepF) had to be immobilized on a chip. His-tagged SeSepF was then immobilized on a Ni-NTA biosensor chip. The dissociation constant (Kd) of SeFtsZ with SeSepF in the absence and presence of GTP were 1.04 and 53.9 μM, respectively (Fig. 2*A*). The interaction in the presence of GDP showed a similar signal to that in the absence of GTP (Fig. 2*A* apo). Next, we measured the interaction between the SeFtsZ and SeSepF mutants. When L272 of FtsZ is replaced with E, the mutant is reduced to polymerize and lose GTPase activity *in E. coli*, and when G109 and G116 of SepF are replaced with R and S, respectively, these SepF mutants have decreased interaction with FtsZ in *B. subtilis* (7, 18). L272 of FtsZ and G109 and G116 of SepF in *B. subtilis* correspond to L272 of SeFtsZ and G116 and G123 of SeSepF (Fig. S1). The binding affinity of $SeFtsZ^{L272E}$ with SeSepF was not affected in the absence or presence of GTP (Kd = 0.98 μM and 0.7 μM) (Fig. 2*B*). The concentration-dependent signal of SeFtsZ did not increase in the sensor immobilized with $SeSepF^{G116R}$ and $SeSepF^{G123S}$ mutants (Fig. 2, *C* and *D*), indicating that the interaction between SeFtsZ and SeSepF mutants was lost due

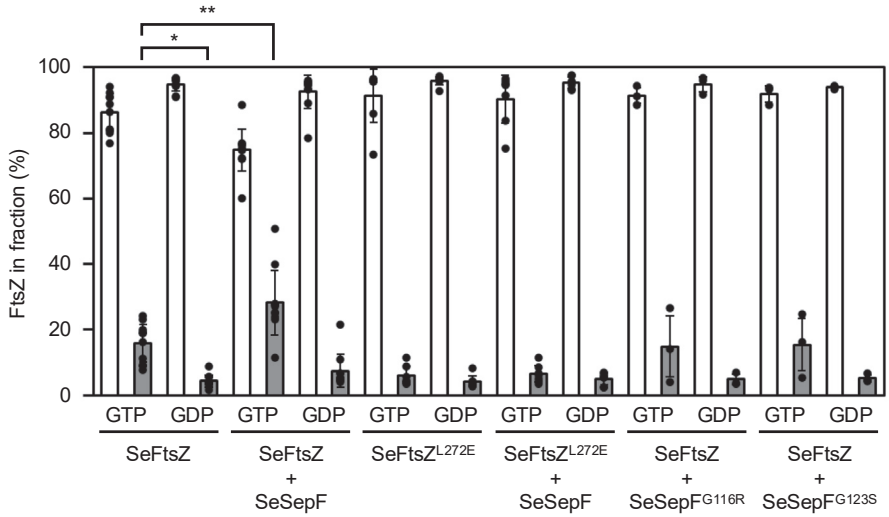

Figure 1. Sedimentation assay of SeFtsZ polymer. SeFtsZ (12 μM) was polymerized with 2 mM GTP or GDP. The amount of protein was estimated using densitometric analysis of CBB-stained SDS-PAGE gels (12%). All the experiments were carried out at least three times and all the data points are superimposed on the bar graph. Statistical significance was assessed using the Student's *t* test: *p = 0.002, **p = 0.004.

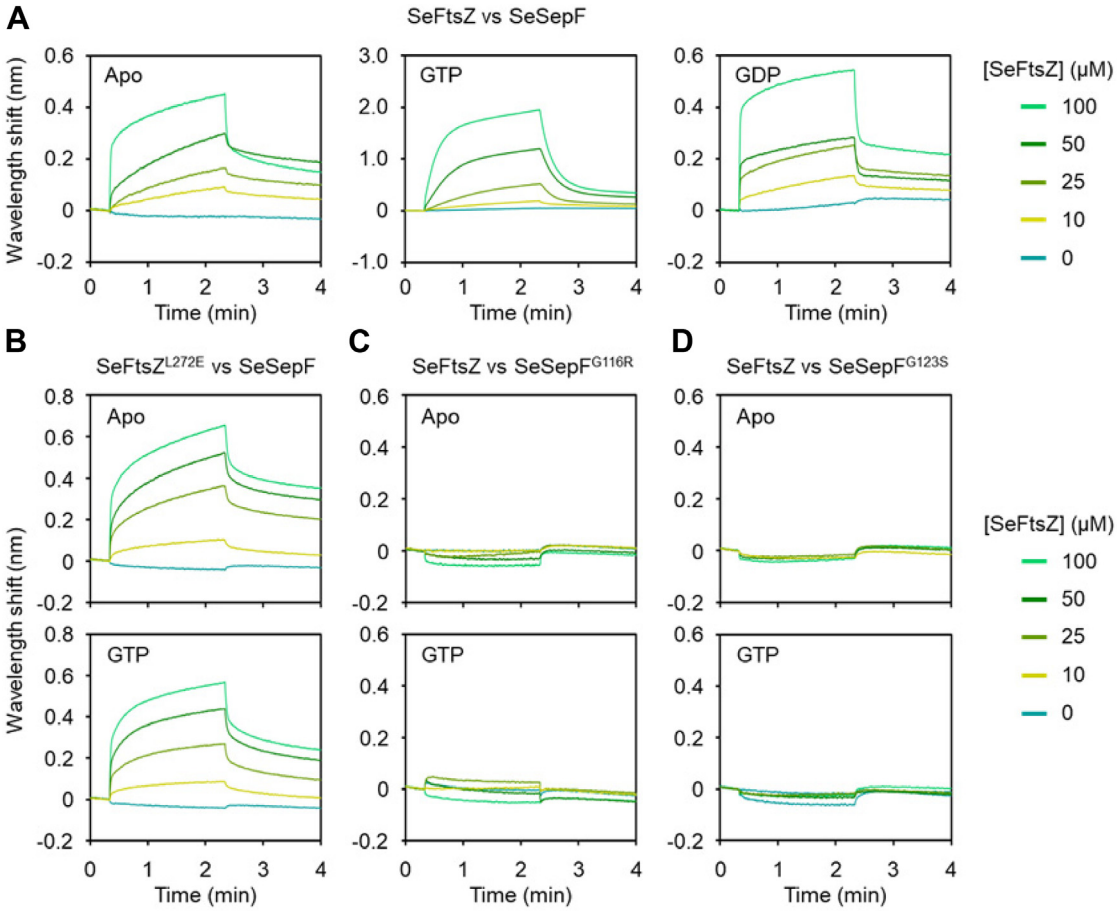

Figure 2. Interaction between SeFtsZ and SeSepF. Binding analysis of SeFtsZ and SeFtsZ^{L272E} mutant with SeSepF and SeSepF mutants was conducted using Bio-layer interferometry. SeSepF (*A* and *B*), SeSepF^{G116R} (*C*), SeSepF^{G123S} (*D*) immobilized on the sensor chip were ligands. The concentrations of SeFtsZ (*A*, *C*, *D*) and SeFtsZ^{L272E} (*B*) mutant, which are the analytes.

to the mutations. The dissociation constant of interaction between SeFtsZ and SeSepF was 1.13 μM as that of *Mycobacterium tuberculosis* (41).

SeFtsZ^{L272E} did not polymerize under any of the conditions (Fig. 1). SeSepF mutants (SeSepF^{G116R} and SeSepF^{G123S}) were tested for polymerization. The amount of SeFtsZ in the pellet fraction did not increase, regardless of the presence of GTP or SeSepF (Fig. 1). These results indicate that SeSepF promotes SeFtsZ polymerization through direct interactions.

Observation of Spiroplasma *FtsZ filaments*

Next, we observed the structures formed by polymerized SeFtsZ. Polymerized SeFtsZ was imaged using electron microscopy (EM). The structures composed of SeFtsZ were thin, short filaments (Fig. 3*A*). Some filaments are curved into partial circles. The width of the filament was approximately 5.7 ± 1.2 nm (Fig. 3*B*), with an inner diameter of the circular structure of 50 to 100 nm. The SeFtsZ polymer incubated with SeSepF formed mostly thin, short filaments, and rarely formed some long, thick bundles (Fig. 3, *C* and *D*). The SeFtsZ^{L272E} mutant did not form filaments or bundles despite the presence or absence of SeSepF (Fig. S2, *A* and *B*). Purified SepF from *B. subtilis* forms tubular structures under neutral pH conditions and ring structures under basic pH (18, 20). We determined whether SeSepF formed any characteristic structures. The structures of SeSepFs were imaged using EM. No SeSepF rings or tubules were observed at neutral pH (Fig. S2*C*). The fact that SepF mutants which impair the ring formation of SepF do not bundle FtsZ in *B. subtilis* (17) would explain why we rarely observed bundles of SeFtsZ even in the presence of SeSepF.

The GTPase activity of Spiroplasma *FtsZ*

Next, we analyzed the effects of SeSepF on the GTPase activity of SeFtsZ. SeFtsZ hydrolysis was determined based on the amount of inorganic phosphate. GTP (1 mM) was added to 12 μM SeFtsZ, and the absorbance (OD_{620}) of the solution was measured for 60 min. The amount of inorganic phosphate in the reaction solution increased for 20 min after adding GTP. The GTPase activity of SeFtsZ was 0.16 ± 0.03 Pi/FtsZ/min (Fig. 4). The GTPase activity of SeFtsZ was measured in the presence of SeSepF. SeSepF slightly increased the GTPase activity of SeFtsZ to 0.27 ± 0.03 Pi/FtsZ/min (Fig. 4). The SeFtsZ^{L272E} mutant did not exhibit an increase in the amount of inorganic phosphate in the reaction solution after 60 min (Fig. 4). The GTP hydrolysis of SeFtsZ was lower than *E. coli* and *B. subtilis* FtsZ. In *B. subtilis*, SepF stabilizes FtsZ filaments and decreases GTPase activity (16). While SeSepF promoted the polymerization of SeFtsZ (Fig. 1), it did not have

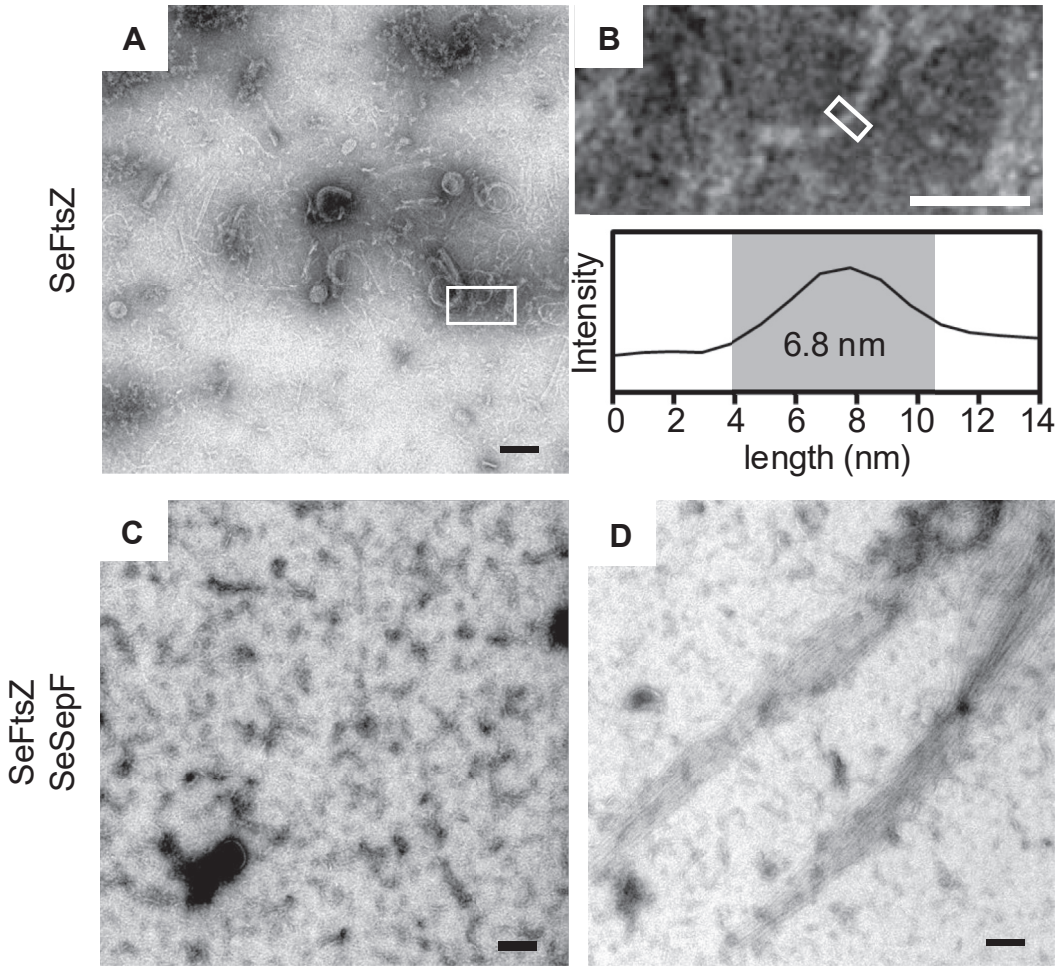

Figure 3. Electron microscope image of polymerized SeFtsZ. *A*, SeFtsZ filaments in the absence of SeSepF. *B*, magnified image of the area indicated by the boxed regions in panel A. The diameter of filaments was estimated from the image intensity measured along the long axis of the area indicated by the box. *C and D*, SeFtsZ filaments and bundles in the presence of SeSepF. Scale bars in *A*, *C*, and *D* are 100 nm. Scale bar in B is 50 nm.

a significant effect on GTPase activity. This suggests that, unlike in *B. subtilis*, SeSepF can promote the polymerization of SeFtsZ but contributes little to its stabilization.

Localization and structure of Spiroplasma *FtsZ in* E. coli

In general, FtsZ polymers form the Z ring at cell division sites. However, the ring-like structure of SeFtsZ in *S. eriocheiris* cells has not been reported. Herein, SeFtsZ formed a Z-ring in living cells; however, a genetic manipulation technique has not been established for *Spiroplasma*. Since *S. eriocheiris* is an obligate anaerobic bacterium, its cultivation is difficult; even if cultured, its growth rate is very slow. Therefore, it is difficult to observe the Z ring in *S. eriocheiris* cells. Previously, we successfully produced FtsZ derived from *Arabidopsis* chloroplasts in *E. coli* and observed ring-like structures, indicating that *E. coli* cells can form Z-rings derived from other species (42). Hence, in this study, we observed SeFtsZ localization in *E. coli* (Fig. 5). Since FtsZ interacts with other cell division proteins through its C-terminal region, this region may be critical for SeFtsZ function. Therefore, the monomeric superfolder GFP (msfGFP) was fused to the N-terminus of SeFtsZ. When msfGFP-SeFtsZ was produced in *E. coli*, it formed foci instead of ring-like structures (Fig. 5*B*). Notably, cells carrying an empty vector did not elongate (Fig. 5*A*), whereas cells producing SeFtsZ became filamentous (Fig. 5*B*). These results suggest that SeFtsZ does not assemble into the Z ring of *E. coli*. Next, msfGFP-SeFtsZ was coproduced with SeSepF in *E. coli* cells. msfGFP-SeFtsZ formed ring-like structures and msfGFP-SeFtsZ was excluded from the cell poles (Fig. 5*C*). The msfGFP-SeFtsZ^{L272E} mutant neither

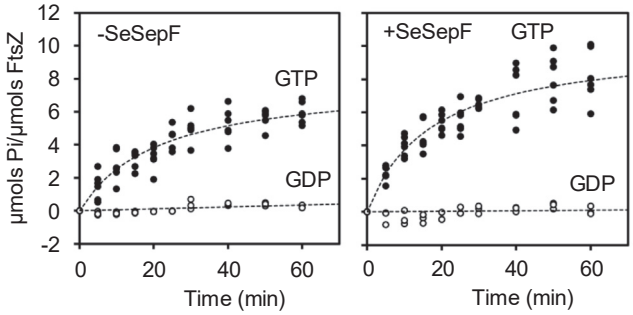

Figure 4. GTP hydrolysis during SeFtsZ polymerization. SeFtsZ (12 µM) polymerized with 1 mM GTP. The reactions in the absence of SeSepF are shown in the *upper panel*, and those in the presence of SeSepF are shown in the *lower panel*. SeFtsZ^{L272E} (12 µM) incubated in the absence or presence with 1 mM GTP.

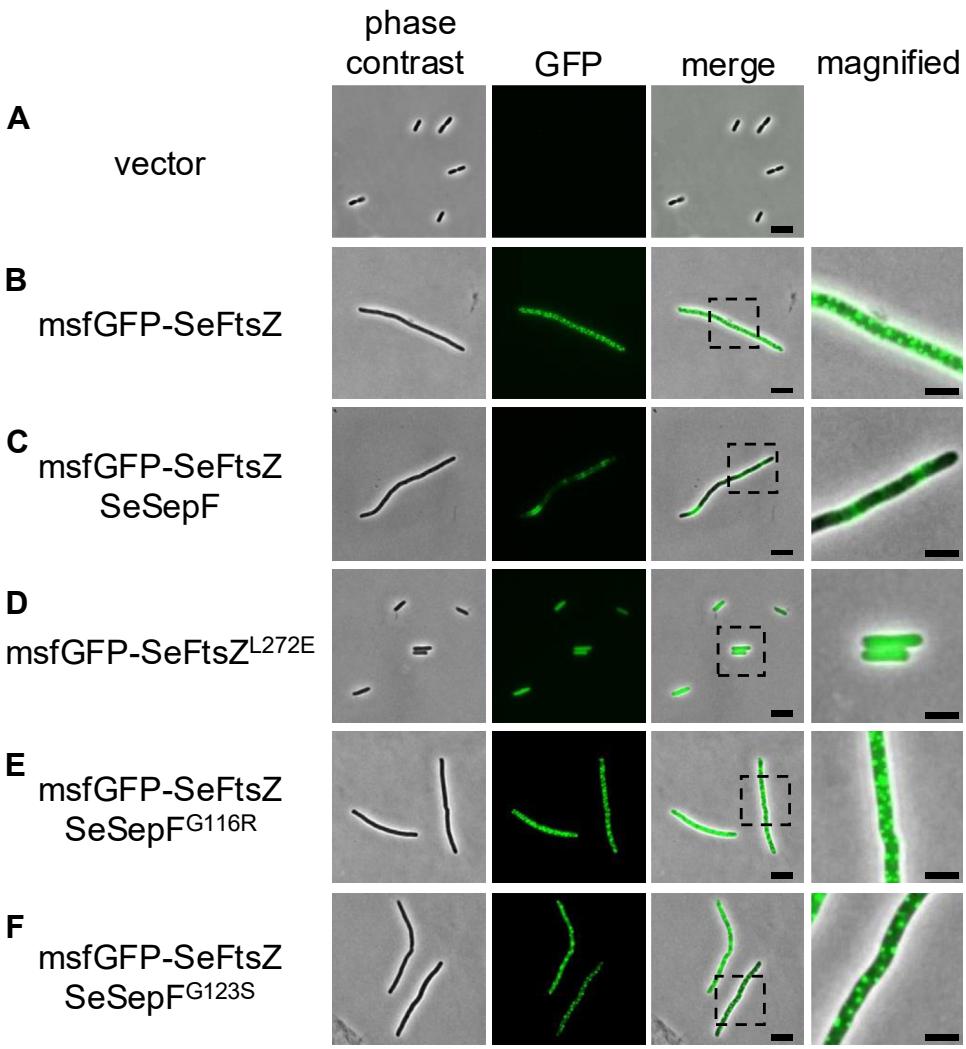

Figure 5. Localization of SeFtsZ in Rod-shaped *E. coli*. *A*, MG1655 with introduced vector. *B*, the msfGFP-SeFtsZ focus formation in MG1655. *C*, The msfGFP-SeFtsZ formed a ring structure in MG1655 producing SeSepF. *D*, The msfGFP-SeFtsZ^{L272E} diffused in the cytoplasm in the presence of SeSepF. *E* and *F*, the msfGFP-SeFtsZ formed a focused structure in MG1655 producing SeSepF mutant. The magnified cell is shown in the *right panel*. Scale bars in regular size pictures and magnified images are 2 μm and 1 μm, respectively.

formed foci nor inhibited cell division (Fig. 5*D*). SeSepF^{G116R} and SeSepF^{G123S} mutants did not affect the localization of msfGFP-SeFtsZ foci, similar to those of msfGFP-SeFtsZ without SeSepF (Fig. 5, *B*, *E* and *F*). To confirm whether msfGFP-SeFtsZ forms ring-like structures in a SepF-dependent manner, we analyzed the localization of SeFtsZ in three dimensions, and only msfGFP-SeFtsZ clusters were observed; in the presence of SepF, ring-like structures of msfGFP-SeFtsZ were observed (Fig. S3). Collectively, SeFtsZ polymerized and formed cluster-like foci within living *E. coli* cells and possibly interacted with SeSepF to form ring-like structures. The inhibition of cell division in *E. coli* is thought to be caused by interacting with endogenous cell division proteins in *E. coli* and/or inhibiting a turn-over of *E. coli* FtsZ by SeFtsZ.

Localization of Spiroplasma *FtsZ in* E. coli *L-forms*

msfGFP-SeFtsZ formed ring-like structures in rod-shaped cells. However, the production of msfGFP-SeFtsZ and SeSepF inhibited cell division in cell-walled *E. coli*. The cell wall may affect the contraction of rings containing msfGFP-SeFtsZ. Therefore, we analyzed the localization of msfGFP-SeFtsZ in cell wall-deficient L-form cells and the division of L-forms that produce msfGFP-SeFtsZ (Fig. 6*A*). When msfGFP-SeFtsZ was produced in the L-form *E. coli*, foci were observed in the cytoplasm. The msfGFP-FtsZ focal point was eventually polymerized and extended. The growth rate of SeFtsZ filaments was 14 ± 6 nm/min (N = 10). SeFtsZ filaments interacted with each other and formed long filaments or branches. Ring- and tube-like SeFtsZ structures were also observed. The average diameter of the msfGFP-SeFtsZ ring had an outer diameter of 500 ± 75 nm and an inner diameter of 215 ± 57 nm. These structures were unlikely to anchor to the cell membrane and did not control the division of L-form cells. The *E. coli* FtsZ ring has a diameter of 1.0 μm (43). The widths of *S. eriocheiris* and *E. coli* are roughly 200 and 1 μm, respectively, suggesting that the curvature of FtsZ filaments depended on the bacterial cell size (44). Next, msfGFP-SeFtsZ

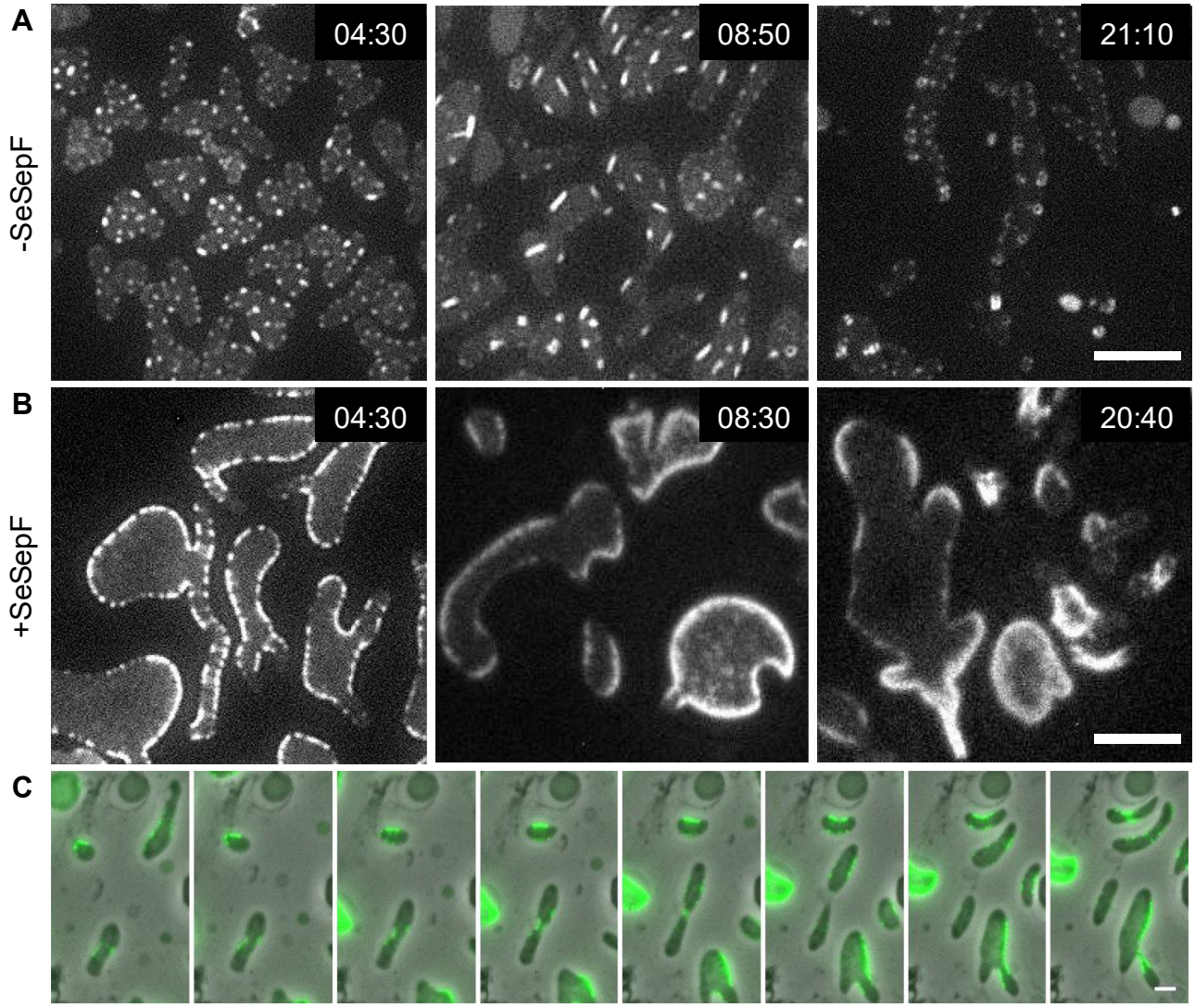

Figure 6. Localization of SeFtsZ in L-form *E. coli*. Time-lapse image showing the msfGFP-SeFtsZ behavior. Cells were grown in NB/MSM medium containing 400 μg/ml Fosfomycin and 0.2% arabinose. *A*, the msfGFP-SeFtsZ filaments elongated and formed the rings in MG1655. *B*, the msfGFP-SeFtsZ localized at the cell membrane in MG1655 producing SeSepF. Scale bar: 5 μm. *C*, time lapse images of cell division in L-form. L-form divided at the localized portion of the msfGFP-SeFtsZ. Scale bar: 2 μm.

and SeSepF were co-produced in L-form cells (Fig. 6*B*). msfGFP-SeFtsZ localized to the cell membrane and formed a ring-like structure. The msfGFP-SeFtsZ ring was not observed in L-form cells where the cell was relatively wide but appeared in the narrow part of the cell (Fig. 6*C*). However, SeSepF seemed not to promote cell division of ameba-like L-forms.

Discussion

Most studies on bacterial cell division have been conducted on cell-walled bacteria, such as *E. coli* and *B. subtilis*. However, there have been limited studies on cell division in bacteria without cell walls (37, 38, 45). The *ftsZ* gene is widely conserved in almost all bacteria, with or without cell walls. Therefore, we predict that FtsZ is important for cell division irrespective of the presence or absence of a cell wall. However, the mechanism behind the involvement of FtsZ in cell division in bacteria lacking a cell wall and the biochemical characteristics of FtsZ in these bacteria are still unknown. Herein, we report the biochemical characteristics of FtsZ in *Spiroplasma*.

The GTPase activity of FtsZ

The GTPase activity of *E. coli* and *B. subtilis* FtsZ are 2.1 Pi/FtsZ/min and 0.8 Pi/FtsZ/min, respectively (39). The GTPase activity of SeFtsZ was 0.2 ± 0.04 Pi/FtsZ/min (Fig. 4). Although SeFtsZ contains conserved amino acids essential for GTP binding and hydrolysis, its GTPase activity is lower than that of *E. coli* and *B. subtilis* FtsZ, which is possibly attributed to the phenylalanine residue at position 226 in SeFtsZ. This residue is predicted to affect conformational changes in FtsZ (46). $SeFtsZ^{F226M}$ had increased GTPase activity (0.24 ± 0.02 Pi/FtsZ/min) (Fig. S4). Low GTPase activity indicates two possibilities: weak hydrolysis of FtsZ or weak interactions with FtsZ. FtsZ, which has a weak hydrolytic ability, remains bound to

GTP and is less likely to depolymerize. In contrast, FtsZ, which weakly interacts with GTP, was less polymerized.

Structures of FtsZ filaments

Previous electron microscopy observations have shown that FtsZ filaments of *E. coli* and *B. subtilis* are formed at 4 to 5 nm wide (47, 48). The width of the SeFtsZ filaments (5.7 ± 1.2 nm) we measured was similar in value. In addition, the filament length was shorter than that of *E. coli* and *B. subtilis*. These short filaments suggest that SeFtsZ does not easily interact with GTP. The SeFtsZ filaments formed ring structures. The ring structures with a diameter of ∼300 nm and ∼200 nm were also observed by EM in *E. coli* and *B. subtilis* FtsZ, respectively (49–51). The diameter of the ring formed by SeFtsZ is smaller than these FtsZ. Therefore, it may be that the ring of SeFtsZ can only be formed in thin cells.

Effects of SepF for FtsZ polymerization in Spiroplasma

A previous study reported that *B. subtilis* SepF reduced the GTPase activity of FtsZ by stabilizing FtsZ filaments (16). It is believed that the stabilization of FtsZ filaments inhibits FtsZ depolymerization, and the reduction of the FtsZ monomer prevents new polymerization. In this study, we showed that SeSepF promoted the polymerization of SeFtsZ but did not affect its GTPase activity, suggesting that SeSepF did not reduce SeFtsZ depolymerization. In *B. subtilis*, the SepF ring controls the alignment and bundling of FtsZ filaments (17, 18, 20). In contrast, we did not observe the ring-like structure of SeSepF by EM. A sequence alignment was performed using SepF from 7 bacteria (Fig. S1). The residues (G116 and G123 in SeSepF) that are important for interaction with FtsZ are highly conserved. SeSepF is shorter than that of other bacteria, and it lacks G135 of SepF in *B. subtilis* that are important for ring formation (17). In *Corynebacterium glutamicum*, T142 of SepF, which corresponds to G135 of *B. subtilis*, inhibits self-interaction (Fig. 7*B*) (52). The predicted structure of the SeSepF dimer in AlphaFold2 was different from that of the SepF dimer in *B. subtilis* and was similar to the structure of *C. glutamicum* (Fig. 7, *A* and *D*). In *Staphylococcus aureus*, the important residue of SepF for the ring formation is conserved and the predicted structure was similar to the structure of *B. subtilis* (Figs. 7*C* and S1). We showed that SeFtsZ monomers interacted more strongly with SeSepF than the polymers. The critical concentration required for FtsZ filament formation is higher in *E. coli* than in *Spiroplasma melliferum* (46). Due to the high critical concentration, several SeFtsZ monomers were present around the polymerized SeFtsZ. Since SeSepF easily

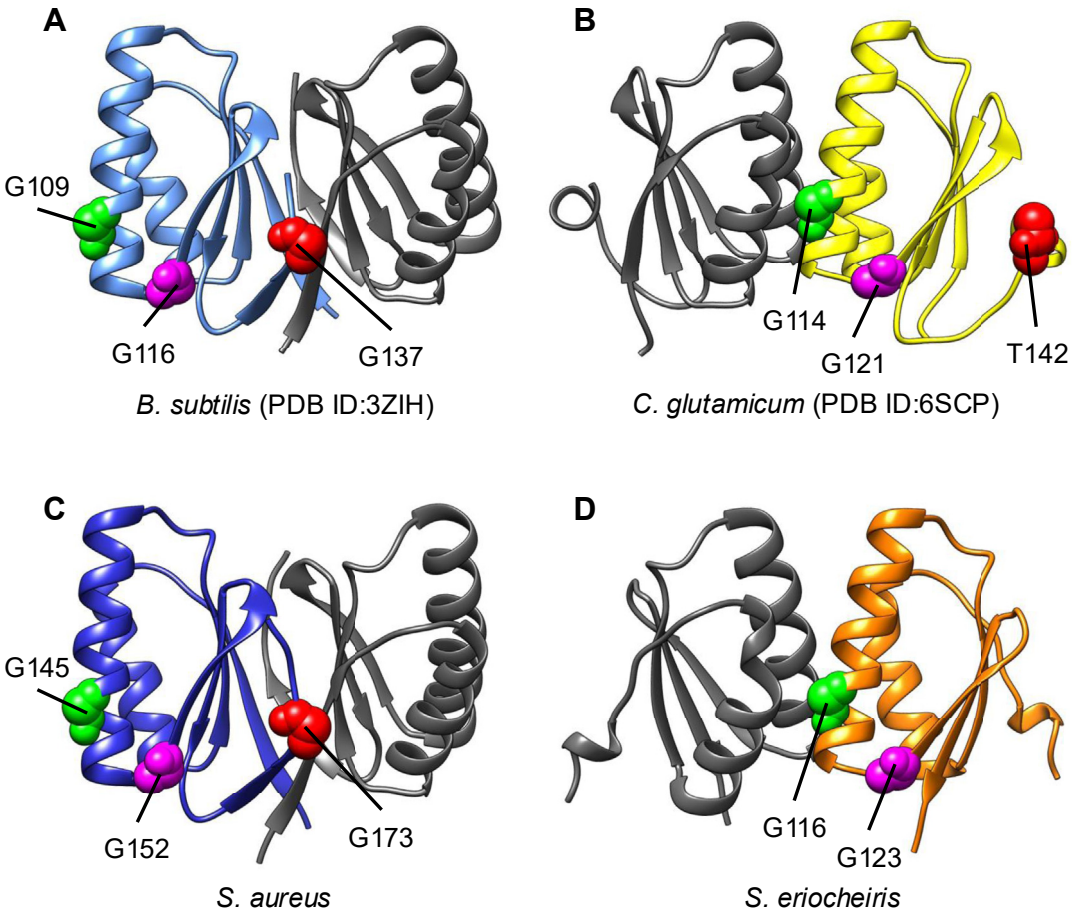

Figure 7. 3D structural model of SepF dimer. *A*, crystal structure of *B. subtilis* SepF dimer (PDB 3ZIH). *B*, crystal structure of *C. glutamicum* SepF dimer (PDB 6SCP). *C and D*, *S. aureus* SepF dimer and SeSepF dimer predicted by AlphaFold2. The highly conserved residues important for interaction with FtsZ are shown (see Fig. S1). The pLDDT value of the predicted models for the core domain of SepF was over 80.

interacts with the SeFtsZ monomer, the release of SeSepF from the SeFtsZ filaments is facilitated, leading to the formation of unstable SeFtsZ filaments.

Cell division of S. eriocheiris

A previous study reported that Mollicutes FtsZ produced in *E. coli* localizes to the cell pole and inhibits cell division (53, 54). Here, we report the movement of SeFtsZ in *E. coli* L-form cells, in which *E. coli* FtsZ does not function. SeFtsZ formed ring- and tube-like structures in L-form cells but did not constrict the cell membrane. Next, we showed that when SeFtsZ and SeSepF were coproduced in L-form cells, SeFtsZ localized to the cell membrane and formed ring-like structures. Ring-like structures constricted cell membranes. The SeFtsZ ring was similar to that of *E. coli* FtsZ when produced in liposomes (32, 55, 56). Our findings also showed that SeFtsZ formed Z rings in a SepF-dependent manner in *E. coli* cells. To our knowledge, this is the first report of Z-rings derived from Mollicutes. However, the SeFtsZ ring may require a physical force to separate the cell membrane. The motility of *Mycoplasma* is involved in the cell division process (57, 58). *S. eriocheiris* may also divide using physical forces generated by swimming motility, and SeFtsZ determines the division sites by narrowing a part of the cell.

Experimental procedures

Bacterial strains and plasmid constructions

E. coli MG1655 is the wild-type strain (59). *E. coli* Rosetta (DE3) cells were used for protein production. *Spiroplasma* genomic DNA was purified using the Wizard Genomic DNA Purification Kit (Promega, Madison, WI, USA). The *ftsZ* and *sepF* genes were amplified using *Spiroplasma* genomic DNA as a template. The TGA codon in *SeftsZ* and *SesepF* was changed to a TGG codon for expression in *E. coli*. *SeftsZ* and *SesepF* were inserted into the pET28a vector at the NdeI and EcoRI sites, yielding pSP2 and pSP3, respectively. SeFtsZ and SeSepF mutants were generated by site-directed mutagenesis using polymerase chain reaction (PCR). $SeftsZ^{L272E}$, $SeftsZ^{F226M}$, $SesepF^{G116R}$, and $SesepF^{G123S}$ were inserted into the NdeI and EcoRI sites of a vector plasmid pET28a, yielding pSP71, pSP98, pSP68, and pSP69, respectively. SeFtsZ and SeSepF mutants were created by replacing pSP71, and pSP68, pSP69 with pSP27. pBAD24 and pBAD33 were excised using ClaI-HindIII (60). The fragment containing multiple cloning sites of pBAD24 was replaced with the corresponding fragment of pBAD33, and the resulting plasmid was named pBAD33-MCS3 (pRU1276). $SeftsZ^{L272E}$, $SesepF^{G116R}$, and $SesepF^{G123S}$ were inserted into the EcoRI and PstI sites of pBAD33-MCS3 to yield pSP89, pSP90, and pSP91, respectively. The PstI-ScaI fragment of pDSW208 was replaced with the corresponding fragment of pDSW207 (61), yielding pRU1565. msfGFP was amplified using RU1514 ($mreB\text{-}msfGFP^{SW}$) as a template, and the PCR product was designed to carry EcoRI and SacI sites at its 5′ and 3′ ends. The PCR products were digested with EcoRI and SacI and inserted into the corresponding site of pRU1565 to yield pRU1563. *msfGFP* was amplified using pRU1563 as the template. *msfGFP* fragment that contains the overlap sequence at the 3′ end fused to *SeftsZ* by PCR. The *gfp-SeftsZ* and *gfp-SeftsZ-SesepF* were inserted into the EcoRI and PstI sites of pBAD33-MCS3 to yield pSP23 and pSP27, respectively. When necessary, antibiotics were added at the following concentrations: 50 μg/mL kanamycin, 20 μg/mL chloramphenicol, and 100 μg/mL ampicillin.

Protein purification

Rosetta (DE3) strains carrying a plasmid encoding *SeftsZ*, *SesepF*, or their mutants were grown in an LB medium containing chloramphenicol and Kanamycin at 37 °C until the OD_{600} reached 0.6. Then, 100 μM isopropyl-β-D-1-thiogalactopyranoside (IPTG) was added to the culture to induce expression of *SeftsZ* or *SesepF*, and cells were incubated for 13 h at 25 °C. The cells were collected by centrifugation at 7000×*g* at 4 °C. The pellet was resuspended in a binding buffer (20 mM Tris-HCl pH 7.4, 500 mM NaCl) and sonicated. The lysate was centrifuged at 22,000×*g* for 20 min at 4 °C. The supernatants were passed through a 0.22-μm filter. The sample solutions were loaded onto a HisTrap HP column in an ÄKTA pure 25 (Cytiva, Tokyo, Japan). The column was washed with binding buffer and eluted with a linear gradient of 10 to 500 mM imidazole in the binding buffer. The eluted fractions were separated using SDS-PAGE (12%), followed by CBB staining. His tags were removed using a Thrombin Cleavage Capture Kit (Merck).

Sedimentation assay

The purified SeFtsZ was mixed with or without SeSepF in a polymerization buffer (50 mM Tris-HCl pH 7.4, 100 mM KCl, 10 mM $MgCl_2$, 1 mM GTP or GDP) and incubated for 30 min at 25 °C. The final concentration of SeFtsZ and SeSepF were 12 μM. The polymerized SeFtsZ was centrifuged at 4 °C for 15 min at 350,000×*g*. The pellet and supernatant fractions were analyzed using SDS-PAGE, followed by CBB staining.

Bio-layer interferometry

Protein–protein interactions were measured using the Octet N1 system (Sartorius). His-SeFtsZ and His-SeSepF were diluted in BLI buffer (50 mM Tris-HCl pH 7.4, 100 mM KCl, 10 mM $MgCl_2$, 0.02% Tween-20). At the loading step, 10 μg/ml His-SeFtsZ and His-SeSepF were immobilized to the Ni-NTA biosensor tips. The sensor tip was dipped into different concentrations of SeFtsZ (0–100 μg/ml) for the association step and moved into the BLI buffer for the dissociation step. The data were analyzed using Octet N1 software.

Electron microscopy

Polymerized SeFtsZ was placed on carbon-coated glow-discharged grids for 5 min at room temperature. After removing the solution, grids were stained with 2% uranyl acetate. The images were acquired using a JEM1010 EM (JEOL)

equipped with a FastScan-F214(T) charge-coupled device camera (TVIPS).

GTP hydrolysis assay

The GTPase activity of SeFtsZ was measured using a malachite green assay. Purified SeFtsZ was incubated with 1 mM GTP at 25 °C. GTP hydrolysis of SeFtsZ was terminated at various reaction times, and inorganic phosphate (Pi) levels were detected using malachite green. The absorbance was measured at 620 nm using a microplate reader. Phosphate concentrations were determined using a phosphate standard curve.

Microscopic observation

MG1655 cells producing GFP-SeFtsZ with or without SeSepF were grown to log phase in L medium. Cells were observed using an Axio Observer (Zeiss), and sectioning images were captured along the z-axis at 0.27 mm intervals and treated using a deconvolution algorithm. MG1655 cells producing GFP-SeFtsZ with or without SeSepF were grown in NB/MSM medium (0.1% Lab-Lemco powder, 0.2% Yeast extract, 0.5% Peptone, 0.5% NaCl, 40 mM $MgCl_2$, 1 M sucrose, 40 mM maleic acid, pH 7.0) at 30 °C until OD_{600} reached 0.4. The cell suspension was loaded onto a CellASIC ONIX B04 A microfluidic plate (Merck). The air and liquid in the chamber were replaced with nitrogen gas and NB/MSM medium supplemented with 300 μg/ml penicillin G, respectively. Microfluidic plates were observed using a phase-contrast microscope (Zeiss). The microscopic images were analyzed using Fiji (NIH) or Zen (Zeiss).

Data availability

The data supporting the conclusions of this article will be made available by the authors.

Supporting information—This article contains supporting information.

Acknowledgments—We thank Risa Ago for constructing a plasmid pBAD33-MCS3 (pRU1276). We thank all members of the Shiomi Lab for their helpful discussions and suggestions.

Author contributions—T. K. and D. S. conceptualization; T. K., Y. O. T., and D. S. methodology; T. K., Y. O. T., and D. S. validation; T. K. formal analysis; T. K., Y. O. T. investigation; T. K., Y. O. T., M. M. and D. S. data curation; T. K. and D. S.writing–original draft; T. K., Y. O. T., M. M., and D. S. writing–review & editing; T. K., Y. O. T., M. M., and D. S. visualization. M. M. and D. S. funding acquisition; D. S. supervision; D. S. project administration.

Funding and additional information—This work was supported by JST CREST (grant number JPMJCR19S5) and the Rikkyo University Special Fund for Research.

Conflict of interest—The authors declare that they have no conflicts of interest with the contents of this article.

Abbreviations—The abbreviations used are: CBB, Coomassie brilliant blue; EM, electron microscope; Kd, dissociation constant; msfGFP, monomeric superfolder GFP; PBPs, penicillin-binding proteins; Pi, inorganic phosphate.

References

1. Battaje, R. R., Piyush, R., Pratap, V., and Panda, D. (2023) Models versus pathogens: how conserved is the FtsZ in bacteria? *Biosci. Rep.* **43**, BSR20221664
2. Löwe, J., and Amos, L. A. (1998) Crystal structure of the bacterial cell-division protein FtsZ. *Nature* **391**, 203–206
3. Cohan, M. C., Eddelbuettel, A. M. P., Levin, P. A., and Pappu, R. V. (2020) Dissecting the functional contributions of the intrinsically disordered C-terminal tail of *Bacillus subtilis* FtsZ. *J. Mol. Biol.* **432**, 3205–3221
4. Matsui, T., Han, X., Yu, J., Yao, M., and Tanaka, I. (2014) Structural change in FtsZ induced by intermolecular interactions between bound GTP and the T7 loop. *J. Biol. Chem.* **289**, 3501–3509
5. Nogales, E., Whittaker, M., Milligan, R. A., and Downing, K. H. (1999) High-resolution model of the microtubule. *Cell* **96**, 79–88
6. Redick, S. D., Stricker, J., Briscoe, G., and Erickson, H. P. (2005) Mutants of FtsZ targeting the protofilament interface: effects on cell division and GTPase activity. *J. Bacteriol.* **187**, 2727–2736
7. Li, Y., Hsin, J., Zhao, L., Cheng, Y., Shang, W., Huang, K. C., *et al.* (2013) FtsZ protofilaments use a hinge-opening mechanism for constrictive force generation. *Science* **341**, 392–395
8. Du, S., Pichoff, S., Kruse, K., and Lutkenhaus, J. (2018) FtsZ filaments have the opposite kinetic polarity of microtubules. *Proc. Natl. Acad. Sci. U. S. A.* **115**, 10768–10773
9. Scheffers, D.-J. (2008) The effect of MinC on FtsZ polymerization is pH dependent and can be counteracted by ZapA. *FEBS. Lett.* **582**, 2601–2608
10. Tonthat, N. K., Arold, S. T., Pickering, B. F., Van Dyke, M. W., Liang, S., Lu, Y., *et al.* (2011) Molecular mechanism by which the nucleoid occlusion factor, SlmA, keeps cytokinesis in check. *EMBO. J.* **30**, 154–164
11. Wu, L. J., and Errington, J. (2004) Coordination of cell division and chromosome segregation by a nucleoid occlusion protein in *Bacillus subtilis*. *Cell* **117**, 915–925
12. Bernhardt, T. G., and de Boer, P. A. J. (2005) SlmA, a nucleoid-associated, FtsZ binding protein required for blocking septal ring assembly over chromosomes in *E. coli*. *Mol. Cell.* **18**, 555–564
13. Adams, D. W., Wu, L. J., and Errington, J. (2015) Nucleoid occlusion protein Noc recruits DNA to the bacterial cell membrane. *EMBO. J.* **34**, 491–501
14. Feddersen, H., Würthner, L., Frey, E., and Bramkamp, M. (2021) Dynamics of the *Bacillus subtilis* min system. *mBio* **12**, e00296
15. Haney, S. A., Glasfeld, E., Hale, C., Keeney, D., He, Z., and de Boer, P. (2001) Genetic analysis of the *Escherichia coli* FtsZ·ZipA interaction in the yeast two-hybrid system. *J. Biol. Chem.* **276**, 11980–11987
16. Singh, J. K., Makde, R. D., Kumar, V., and Panda, D. (2008) SepF increases the assembly and bundling of FtsZ polymers and stabilizes FtsZ protofilaments by binding along its length. *J. Biol. Chem.* **283**, 31116–31124
17. Gündoğdu, M. E., Kawai, Y., Pavlendova, N., Ogasawara, N., Errington, J., Scheffers, D.-J., *et al.* (2011) Large ring polymers align FtsZ polymers for normal septum formation. *EMBO J.* **30**, 617–626
18. Duman, R., Ishikawa, S., Celik, I., Strahl, H., Ogasawara, N., Troc, P., *et al.* (2013) Structural and genetic analyses reveal the protein SepF as a new membrane anchor for the Z ring. *Proc. Natl. Acad. Sci. U. S. A.* **110**, E4601–E4610
19. Krupka, M., Cabré, E. J., Jiménez, M., Rivas, G., Rico, A. I., and Vicente, M. (2014) Role of the FtsA C terminus as a switch for polymerization and membrane association. *mBio* **5**, e02221
20. Wenzel, M., Gulsoy, I. N. C., Gao, Y., Teng, Z., Willemse, J., Middelkamp, M., *et al.* (2021) Control of septum thickness by the curvature of SepF polymers. *Proc. Natl. Acad. Sci. U. S. A.* **118**, e2002635118
21. Erickson, H. P., Anderson, D. E., and Osawa, M. (2010) FtsZ in bacterial cytokinesis: cytoskeleton and force generator all in one. *Microbiol. Mol. Biol. Rev. MMBR.* **74**, 504–528
22. Lutkenhaus, J., Pichoff, S., and Du, S. (2012) Bacterial cytokinesis: from Z ring to divisome. *Cytoskelet. Hoboken NJ* **69**, 778–790

23. Meeske, A. J., Riley, E. P., Robins, W. P., Uehara, T., Mekalanos, J. J., Kahne, D., *et al.* (2016) SEDS proteins are a widespread family of bacterial cell wall polymerases. *Nature* **537**, 634–638
24. Taguchi, A., Welsh, M. A., Marmont, L. S., Lee, W., Sjodt, M., Kruse, A. C., *et al.* (2019) FtsW is a peptidoglycan polymerase that is functional only in complex with its cognate penicillin-binding protein. *Nat. Microbiol.* **4**, 587–594
25. Errington, J., Daniel, R. A., and Scheffers, D.-J. (2003) Cytokinesis in bacteria. *Microbiol. Mol. Biol. Rev.* **67**, 52–65
26. Yang, X., Lyu, Z., Miguel, A., McQuillen, R., Huang, K. C., and Xiao, J. (2017) GTPase activity–coupled treadmilling of the bacterial tubulin FtsZ organizes septal cell wall synthesis. *Science* **355**, 744–747
27. McQuillen, R., and Xiao, J. (2020) Insights into the structure, function, and dynamics of the bacterial cytokinetic FtsZ-ring. *Annu. Rev. Biophys.* **49**, 309–341
28. Kocaoglu, O., and Carlson, E. E. (2015) Profiling of β-lactam selectivity for penicillin-binding proteins in *Escherichia coli* strain DC2. *Antimicrob. Agents. Chemother.* **59**, 2785–2790
29. Errington, J., Mickiewicz, K., Kawai, Y., and Wu, L. J. (2016) L-form bacteria, chronic diseases and the origins of life. *Philos. Trans. R. Soc. B Biol. Sci.* **371**, 20150494
30. Mercier, R., Kawai, Y., and Errington, J. (2014) General principles for the formation and proliferation of a wall-free (L-form) state in bacteria. *eLife* **3**, e04629
31. Hayashi, M., Takaoka, C., Higashi, K., Kurokawa, K., Margolin, W., Oshima, T., *et al.* (2024) Septal wall synthesis is sufficient to change ameba-like cells into uniform oval-shaped cells in *Escherichia coli* L-forms. *Commun. Biol.* **7**, 1–13
32. Osawa, M., Anderson, D. E., and Erickson, H. P. (2008) Reconstitution of contractile FtsZ rings in liposomes. *Science* **320**, 792–794
33. Zhang, Z., He, M., Jiang, J., Li, X., Li, H., Zhang, W., *et al.* (2022) First report and comparative genomic analysis of *Mycoplasma capricolum* subsp. *capricolum* HN-B in hainan island, China. *Microorganisms* **10**, 2298
34. Zhang, Z., Jiang, J., He, M., Li, H., Cheng, Y., An, Q., *et al.* (2022) First report and comparative genomic analysis of a *Mycoplasma mycoides* subspecies *capri* HN-A in hainan Island. *Microorganisms* **10**, 1908
35. Lazarev, V. N., Levitskii, S. A., Basovskii, Y. I., Chukin, M. M., Akopian, T. A., Vereshchagin, V. V., *et al.* (2011) Complete genome and proteome of *Acholeplasma laidlawii*. *J. Bacteriol.* **193**, 4943–4953
36. Yokomi, R., Rattner, R., Osman, F., Maheshwari, Y., Selvaraj, V., Pagliaccia, D., *et al.* (2020) Whole genome sequence of five strains of *Spiroplasma citri* isolated from different host plants and its leafhopper vector. *BMC Res. Notes* **13**, 320
37. Lluch-Senar, M., Querol, E., and Piñol, J. (2010) Cell division in a minimal bacterium in the absence of *ftsZ*. *Mol. Microbiol.* **78**, 278–289
38. Pelletier, J. F., Sun, L., Wise, K. S., Assad-Garcia, N., Karas, B. J., Deerinck, T. J., *et al.* (2021) Genetic requirements for cell division in a genomically minimal cell. *Cell* **184**, 2430–2440.e16
39. Król, E., and Scheffers, D.-J. (2013) FtsZ polymerization assays: simple protocols and considerations. *J. Vis. Exp.* https://doi.org/10.3791/50844
40. Mukherjee, A., and Lutkenhaus, J. (1999) Analysis of FtsZ assembly by light scattering and determination of the role of divalent metal cations. *J. Bacteriol.* **181**, 823–832
41. Zhang, H., Chen, Y., Zhang, Y., Qiao, L., Chi, X., Han, Y., *et al.* (2023) Identification of anti-*Mycobacterium tuberculosis* agents targeting the interaction of bacterial division proteins FtsZ and SepFe. *Acta Pharm. Sin. B.* **13**, 2056–2070
42. Irieda, H., and Shiomi, D. (2017) ARC6-mediated Z ring-like structure formation of prokaryote-descended chloroplast FtsZ in *Escherichia coli*. *Sci. Rep.* **7**, 3492
43. Ramirez-Diaz, D. A., García-Soriano, D. A., Raso, A., Mücksch, J., Feingold, M., Rivas, G., *et al.* (2018) Treadmilling analysis reveals new insights into dynamic FtsZ ring architecture. *PLOS Biol.* **16**, e2004845
44. Sasajima, Y., Kato, T., Miyata, T., Kawamoto, A., Namba, K., and Miyata, M. (2022) Isolation and structure of the fibril protein, a major component of the internal ribbon for *Spiroplasma* swimming. *Front. Microbiol.* **13**, 1004601
45. Martínez-Torró, C., Torres-Puig, S., Marcos-Silva, M., Huguet-Ramón, M., Muñoz-Navarro, C., Lluch-Senar, M., *et al.* (2021) Functional characterization of the cell division gene cluster of the wall-less bacterium *Mycoplasma genitalium*. *Front. Microbiol.* **12**, 695572
46. Chakraborty, J., Poddar, S. M., Dutta, S., Bahulekar, V., Harne, S., Srinivasan, R., *et al.* (2024) Dynamics of interdomain rotation facilitates FtsZ filament assembly. *J. Biol. Chem.* **300**, 107336
47. Mingorance, J., Tadros, M., Vicente, M., González, J. M., Rivas, G., and Vélez, M. (2005) Visualization of single *Escherichia coli* FtsZ filament dynamics with atomic force microscopy. *J. Biol. Chem.* **280**, 20909–20914
48. Andreu, J. M., Schaffner-Barbero, C., Huecas, S., Alonso, D., Lopez-Rodriguez, M. L., Ruiz-Avila, L. B., *et al.* (2010) The antibacterial cell division inhibitor PC190723 is an FtsZ polymer-stabilizing agent that induces filament assembly and condensation. *J. Biol. Chem.* **285**, 14239–14246
49. Buske, P. J., and Levin, P. A. (2012) Extreme C terminus of bacterial cytoskeletal protein FtsZ plays fundamental role in assembly independent of modulatory proteins. *J. Biol. Chem.* **287**, 10945–10957
50. Huecas, S., Ramírez-Aportela, E., Vergoñós, A., Núñez-Ramírez, R., Llorca, O., Díaz, J. F., *et al.* (2017) Self-organization of FtsZ polymers in solution reveals spacer role of the disordered C-terminal tail. *Biophys. J.* **113**, 1831–1844
51. Popp, D., Iwasa, M., Narita, A., Erickson, H. P., and Maéda, Y. (2009) FtsZ condensates: an in vitro electron microscopy study. *Biopolymers* **91**, 340–350
52. Sogues, A., Martinez, M., Gaday, Q., Ben Assaya, M., Graña, M., Voegele, A., *et al.* (2020) Essential dynamic interdependence of FtsZ and SepF for Z-ring and septum formation in *Corynebacterium glutamicum*. *Nat. Commun.* **11**, 1641
53. Vedyaykin, A. D., Polinovskaya, V. S., Sabantsev, A. V., Khodorkovskii, M. A., Borchsenius, S. N., and Vishnyakov, I. E. (2017) Influence of FtsZ proteins from some *Mycoplasma* species on the division process in *Escherichia coli* cells. *Cell Tissue Biol* **11**, 389–398
54. Vedyaykin, A. D., Sabantsev, A. V., Khodorkovskii, M. A., Kayumov, A. R., and Vishnyakov, I. E. (2016) Recombinant FtsZ proteins from mollicutes interact with *Escherichia coli* division machinery. *BioNanoScience* **6**, 443–446
55. Osawa, M., and Erickson, H. P. (2013) Liposome division by a simple bacterial division machinery. *Proc. Natl. Acad. Sci.* **110**, 11000–11004
56. Ramirez-Diaz, D. A., Merino-Salomón, A., Meyer, F., Heymann, M., Rivas, G., Bramkamp, M., *et al.* (2021) FtsZ induces membrane deformations via torsional stress upon GTP hydrolysis. *Nat. Commun.* **12**, 3310
57. Balish, M. F. (2014) *Mycoplasma pneumoniae*, an underutilized model for bacterial cell biology. *J. Bacteriol.* **196**, 3675–3682
58. Seto, S., Layh-Schmitt, G., Kenri, T., and Miyata, M. (2001) Visualization of the attachment organelle and cytadherence proteins of *Mycoplasma pneumoniae* by immunofluorescence microscopy. *J. Bacteriol.* **183**, 1621
59. Jensen, K. F. (1993) The *Escherichia coli* K-12 "wild types" W3110 and MG1655 have an *rph* frameshift mutation that leads to pyrimidine starvation due to low *pyrE* expression levels. *J. Bacteriol.* **175**, 3401–3407
60. Guzman, L. M., Belin, D., Carson, M. J., and Beckwith, J. (1995) Tight regulation, modulation, and high-level expression by vectors containing the arabinose P_{BAD} promoter. *J. Bacteriol.* **177**, 4121–4130
61. Weiss, D. S., Chen, J. C., Ghigo, J.-M., Boyd, D., and Beckwith, J. (1999) Localization of FtsI (PBP3) to the septal ring requires its membrane anchor, the Z ring, FtsA, FtsQ, and FtsL. *J. Bacteriol.* **181**, 508–520